

See discussions, stats, and author profiles for this publication at: <https://www.researchgate.net/publication/251528771>

Wettability behaviour of RTV silicone rubber coated on nanostructured aluminium surface

Article in *Applied Surface Science* · May 2011

DOI: 10.1016/j.apsusc.2011.02.049

CITATIONS

26

READS

171

3 authors:



G. Momen

Bombardier

20 PUBLICATIONS 191 CITATIONS

[SEE PROFILE](#)



Masoud Farzaneh

University of Québec in Chicoutimi

472 PUBLICATIONS 5,287 CITATIONS

[SEE PROFILE](#)



R. Jafari

University of Québec in Chicoutimi

26 PUBLICATIONS 335 CITATIONS

[SEE PROFILE](#)

Some of the authors of this publication are also working on these related projects:



Transmission Line Surge Arresters [View project](#)

All content following this page was uploaded by G. Momen on 04 November 2014.

The user has requested enhancement of the downloaded file. All in-text references [underlined in blue](#) are added to the original document and are linked to publications on ResearchGate, letting you access and read them immediately.



Wettability behaviour of RTV silicone rubber coated on nanostructured aluminium surface

Gelareh Momen*, Masoud Farzaneh, Reza Jafari

NSERC/Hydro-Quebec/UQAC Industrial Chair on Atmospheric Icing of Power Network Equipment (CIGELE), and Canada Research Chair on Atmospheric Icing Engineering of Power Networks (INGIVRE), Université du Québec à Chicoutimi (UQAC), Chicoutimi, QC, Canada

ARTICLE INFO

Article history:

Received 10 November 2010
Received in revised form 8 February 2011
Accepted 14 February 2011
Available online 16 March 2011

Keywords:

Superhydrophobicity
Anodising
Supercooled temperature
Silicone rubber
Voltage

ABSTRACT

A nanostructured superhydrophobic surface was elaborated by applying an RTV silicone rubber coating on electrochemically processed aluminium substrates. Study of anodisation voltage on surface morphology showed that higher anodising voltage led to larger pore sizes. Scanning electron microscopy image analysis showed bird's nest and beehive structures formed on anodised surfaces at 50 V and 80 V. Water static contact angle on the treated surfaces reached up to 160° at room temperature. Study of superhydrophobic surfaces at super cooled temperature showed important delayed freezing time for RTV hydrophobic surfaces when compared to non-treated aluminium. However, lower wettability was observed when surface temperature went down from 20 °C to −10 °C. Also, it was found that the capacitance of superhydrophobic surfaces decreased with increasing anodising voltage.

© 2011 Elsevier B.V. All rights reserved.

1. Introduction

In many regions of the world, ice or wet snow accumulation on high voltage overhead transmission lines is one of the major problems faced by utilities, as demonstrated by the ice storms that hit Eastern Canada and Southern China in 1998 and 2008, respectively [1–3].

Recently, superhydrophobic surfaces with a water contact angle (CA) larger than 150° have gained considerable attention because of their various practical applications as coatings on exposed structures such as overhead transmission and distribution lines as well as their substation equipment. Superhydrophobic surfaces prepared by applying low surface energy materials on rough surfaces have shown promising anti-icing performance [4–8]. Furthermore, icephobic surfaces have attracted a great interest compared to de-icing fluid active methods to reduce ice or snow accumulation on high voltage overhead transmission lines [3].

To create micro-nano roughness on an Al surface, several methods including chemical etching in acid [9–11] or alkali solutions [12,13] has been proposed. However, such methods could lead to a corrosion issue. In the present study, anodic aluminium oxide has been proposed as a suitable industrial process that increases resistance to corrosion [14]. Moreover, this method leads to the for-

mation of nano-pore structured films [15,16] which in turn reduce the ice surface contact with the substrate. During the anodising process, several factors are to be taken into account in the formation of thin films, such as anodising temperature, voltage, electrolyte and also anodising time [17]. Indeed, the control of surface roughness is essential in preparing superhydrophobic surfaces.

Room-temperature vulcanized (RTV) silicon rubber coating, due to its low energy surface, offers good water repellency properties and helps prevent continuous water filming on the surface. The coating can be applied by several methods such as dipping, painting, or spraying. Indeed, the liquid polymer layer vulcanizes inside a flexible rubber layer when exposed to moisture in the air [18]. Furthermore, silicone rubber exhibits the ability to restore its hydrophobicity even after a pollution layer has built up on the surface [18,19]. This has been attributed to the diffusion of low molecular weight (LMW) silicone fluid from the coating onto the polluted deposits [19].

In the present study, several anodisation voltages were applied to create different nanostructured surfaces. Superhydrophobic surfaces were provided using RTV silicone rubber coating on the anodised samples. The wettability behaviour of these surfaces was analysed at temperatures ranging from 20 °C to −10 °C. Then, the effect of anodising voltage on the coating capacitance was studied.

2. Experimental

Hand-polished 6061 Al alloy coupons (2.54 cm × 2.54 cm × 0.15 cm) from Rio Tinto Alcan (Mg 1.0, Si

* Corresponding author at: CIGELE/INGIVRE, Département des sciences appliquées, Université du Québec à Chicoutimi, Saguenay, QC, G7H 2B1, Canada.

E-mail address: gmomen@uqac.ca (G. Momen).

URL: <http://www.cigele.ca> (G. Momen).

0.6, Cu 0.28, Cr 0.05, Zn 0.1, Fe 0.25 and Mn 0.15, all in wt%) were used as substrate.

Anodised aluminium were prepared by an electrochemical bath consisting of a 10% (w/w) solution of H_3PO_4 at $T = 18^\circ C$ during 90 min. Prior to the anodisation process, the samples were degreased using an ultrasonic bath of acetone followed by deionised water, each for 5 min. The anodising process was done at anodising voltages of 40 V, 50 V, 60 V and 80 V.

RTV silicone rubber 3-4190 was purchased from Dow corning. This product was selected because it does not contain fillers. First, the RTV silicone rubber was diluted by adding hexane in a volume ratio of 1:12. Then, the solution was deposited on the substrates via a sol-gel spin coating (WS-400B-6NPP spin-coater from Laurel). The spinning speed was set at 3000 rpm (20 s) and 2500 rpm (15 s) for the first and second stages, respectively. Heat treatment of the coatings was done at $85^\circ C$ in air, and was left overnight to remove residual solvents.

The surface morphology of the samples was examined using a LEO field emission scanning electron microscope (FESEM) and an AFM (Digital Nanoscope III by Digital Instruments). Static water contact angle measurements were made using a Kruss DSA 100 goniometer (water droplet volume $\sim 4 \mu l$). Contact angle hysteresis was measured using a common experimental procedure [20]. The samples were placed on a test stage and a double-distilled water droplet was introduced onto the surface through a microsyringe. At least five different measurements were performed on different areas of each sample. The electrical capacitance of the treated samples was measured using an Agilent 4294A impedance analyzer, with frequency ranging from 40 Hz to 2 KHz. The samples analysed were porous aluminium coated with RTV silicone rubber.

3. Results and discussion

3.1. Surface morphology

The effect of anodising voltage on surface morphology was investigated. SEM microphotographs taken for Al anodised samples with three applied voltage are shown in Fig. 1.

The irregular structure and discontinuity was observed for the pores formed at 40 V anodising voltage (Fig. 1a). The pores formed at 50 V were organized as an “hexagonal bird’s nest” structure separated by thinner pore walls, as shown in Fig. 1b. At 80 V, the pores were continuously formed on the surface, becoming more open and deeper, with a “beehive” structure (see Fig. 1c). As anodising voltage was increased, the pores became wider, indicating that the anodisation voltage affects the size and form of the pore. The average pore diameter anodised with 40 V, 50 V and 80 V was around 50 nm, 80 nm and 120 nm, respectively. The development of pore structure was found to be proportional to applied voltage which is consistent with what was reported in [21,22].

The morphology characterizations of anodised Al surfaces were carried out using AFM as shown in Fig. 2. The AFM image obtained for 40 V showed the formation mechanism of porous aluminium oxide film is not well established (see Fig. 2a). As voltage was increased to 50 V and 80 V, good development of porous anodic aluminium oxide was observed (see Fig. 2b and c). These results confirmed the earlier observations by SEM analysis.

3.2. Wettability behaviour at room temperature

Contact angles are the result of the molecular interactions of solid-liquid, liquid-gas, and gas-liquid at the three-phase contact point. The sessile droplet method, which measures the contact angle (CA) of a water droplet on a surface, was used to characterize the wetting property of the surface.

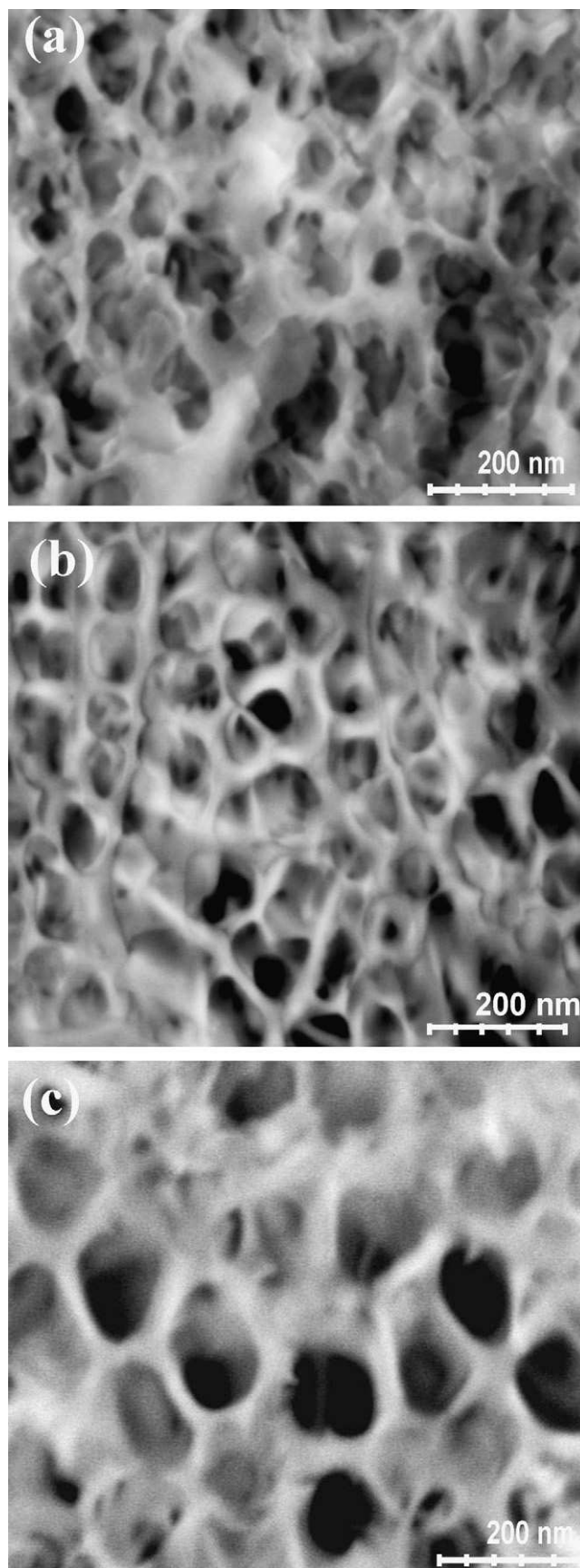


Fig. 1. FESEM micrographs of porous aluminium formed by anodisation at different voltages (a) 40 V, (b) 50 V and (c) 80 V.

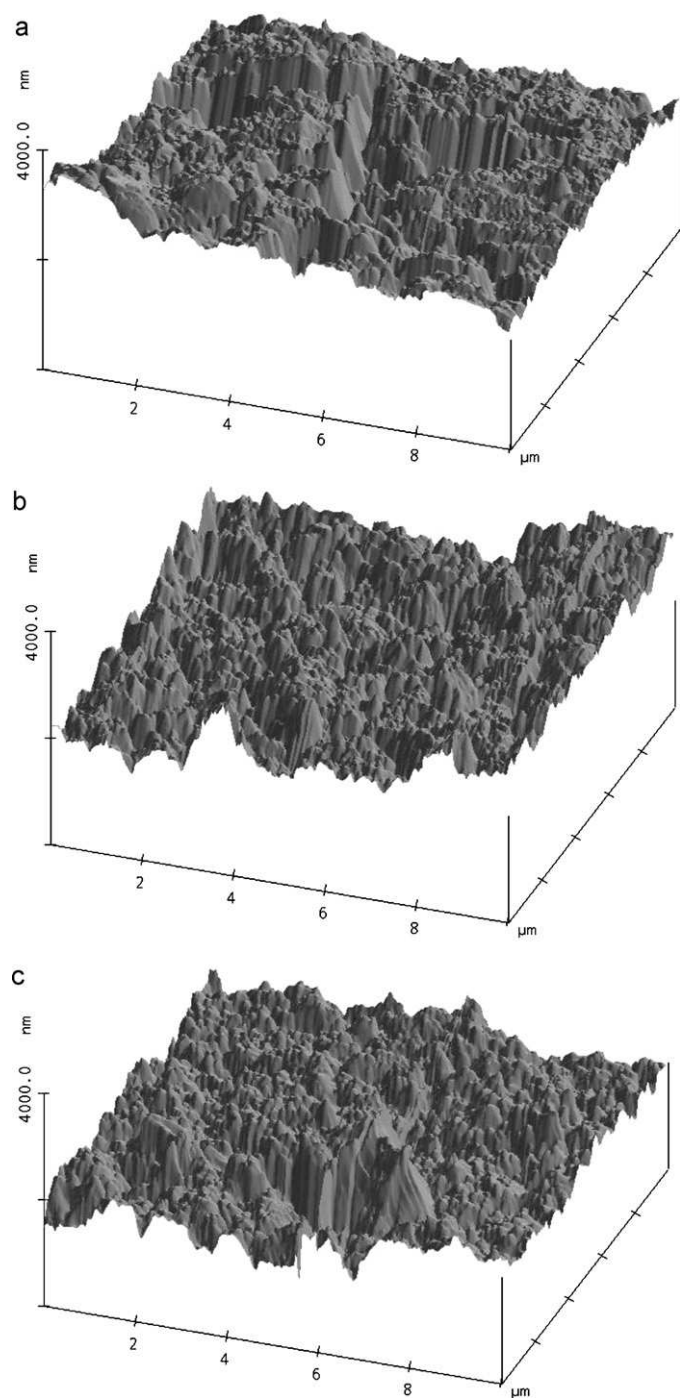


Fig. 2. $10 \times 10 \mu\text{m}$, 3-D tapping mode AFM images of anodised Al at (a) 40 V, (b) 50 V, and (c) 80 V.

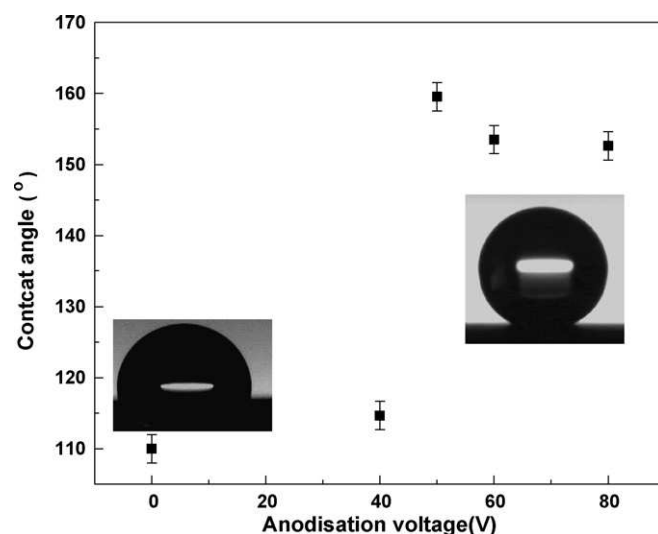


Fig. 3. Static contact angle of nanostructured surfaces as a function of applied voltage.

Variations in static contact angle of RTV silicone rubber coatings deposited on aluminium surfaces as a function of anodisation voltage are shown in Fig. 3. The static water contact angle of a hand-polished Al bar was about $110 \pm 2^\circ$. Application of 40 V anodising voltage resulted in a slight increase of contact angle ($114 \pm 2^\circ$) whereas increasing voltage led to a higher contact angle ($160 \pm 1.2^\circ$) with the surface becoming superhydrophobic.

Applying RTV silicone rubber coating on more anodised surfaces (50 V and more) resulted in superhydrophobic behaviour whereas a 40 V anodised surface with the same coating remained hydrophobic. However, the best wettability was found with 50 V anodising voltage. Otherwise, the created surface roughness at this voltage included an appropriate combination of micro/nano structure (see Fig. 2b).

3.3. Wettability behaviour at supercooled temperature

The study of the water contact angle at supercooled temperature is of prime importance for the development of icephobic superhydrophobic coating [22,23]. For this propose, we carried out CA measurement of samples at temperature as low as -15°C . The Kruss DSA 100 apparatus was fitted with a Peltier cooling element which allowed lowering the substrate temperature down to -30°C .

At -10°C , the freezing time of $4 \mu\text{l}$ water droplets on the superhydrophobic surfaces was longer than 20 min while it was at 4 min at -15°C . Fig. 4 shows the variation in shape of a freezing water droplet ($4 \mu\text{l}$) on a 50 V RTV superhydrophobic surface at -15°C . Droplet crystallization on such surfaces was observed after 4–5 min, which is significantly longer than on a polished aluminium surface (-5 s) or on an RTV-coated hand-polished surface (-11 s).

After 205 s, the droplet shape is starting to expand, showing ice nucleation at the solid–water interface. It was observed that the interface between water and ice kept moving from bottom to top

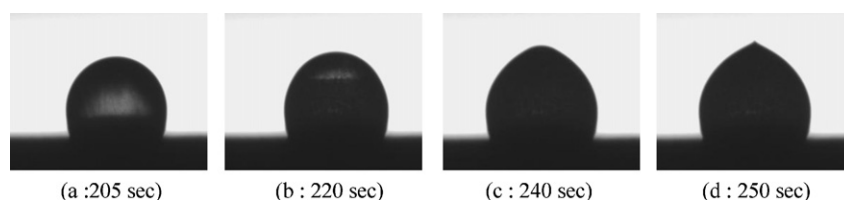


Fig. 4. Image sequences of water droplets ($4 \mu\text{l}$) freezing process on anodised Al at 50 V applied voltage under a constant temperature of -15°C .

Table 1
Contact angles of anodised surfaces as a function of temperature.

| Applied voltage (V) | Temperature (°C) | | | |
|---------------------|------------------|----------|----------|----------|
| | 20 | 0 | −5 | −10 |
| 40 | 114 ± 2° | 108 ± 2° | 102 ± 3° | 98 ± 3° |
| 50 | 160 ± 1° | 149 ± 2° | 138 ± 3° | 125 ± 2° |
| 60 | 150 ± 2° | 147 ± 2° | 131 ± 3° | 118 ± 4° |
| 80 | 152 ± 2° | 146 ± 2° | 132 ± 2° | 116 ± 3° |

during the transient heat conduction after which droplet crystallization occurred completely.

Indeed, entrapped air in the cavities of superhydrophobic surfaces could acts as a thermal barrier between the solid and the liquid delaying freezing time on these surfaces [23].

The wettability of the fabricated surfaces was evaluated for a wide range of temperature. Table 1 listed the static water contact angle of anodised surface at the following temperatures: 20, 0, −5 and −10°C. Each measurement was repeated three times. Wettability of all the surfaces fell with temperature. The descent was more pronounced for superhydrophobic surfaces than hydrophobic ones. The results revealed that the superhydrophobic surfaces became less hydrophobic as surface temperatures went from 20°C to −10°C.

A high static contact angle water droplet deposited on a horizontal surface may remain pinned until the surface is tilted to a considerable angle. Therefore, the static contact angle alone is not sufficient for reflecting the real wettability of a solid surface [15].

Measurement of contact angle hysteresis is also an important criterion to characterize superhydrophobic and icephobic surfaces [4]. The evolution of the water contact angle hysteresis (θ_H) of 50 V RTV superhydrophobic surface as a function of substrate temperature was shown in Table 2. The results showed that by decreasing the temperature of 50 V RTV superhydrophobic surface from 20°C to −10°C, contact angle hysteresis increased from $7 \pm 2^\circ$ to $28 \pm 3^\circ$, respectively.

Indeed, when nanostructured surfaces were exposed to temperatures lower than 0°C, condensed water vapour penetrated into the porosities of coating and water condensation lead to the Cassie–Wenzel regime transition resulting in lower static contact angles and higher contact angle hysteresis [22,23].

3.4. Dielectric characteristic

Among the three physical forces that contribute to ice adhesion, the electrostatic forces have been found to be more dominant [24]. The lower the dielectric constant (ϵ) is, the lower the electrostatic-related adhesion is ($F \propto \epsilon$) [24,25]. According to this relationship, materials with a low dielectric constant would reduce the ice adhesion by reducing the electrostatic interaction.

The dependence of capacitance on anodising voltage as a function of frequency is illustrated in Fig. 5. Low capacitance and consequently low dielectric constant was found for the samples whose pores had been widened. It is interesting to remark that an increase in anodising voltage decreased the capacitance of aluminium. As a matter of fact, the pore became larger (see Fig. 1) and the porosity increased with increasing anodising voltage which in turn leads to more trapped air space and lower capacitance. Otherwise, the superhydrophobic surfaces had low capacitance and consequently low dielectric constant.

Table 2
Contact angles hysteresis of RTV superhydrophobic surface as a function of substrate temperature.

| Temperature (°C) | 20 | 0 | −5 | −10 |
|---------------------------------------|-----------------|------------------|------------------|------------------|
| Contact angle hysteresis (θ) | $7 \pm 2^\circ$ | $15 \pm 3^\circ$ | $20 \pm 4^\circ$ | $28 \pm 3^\circ$ |

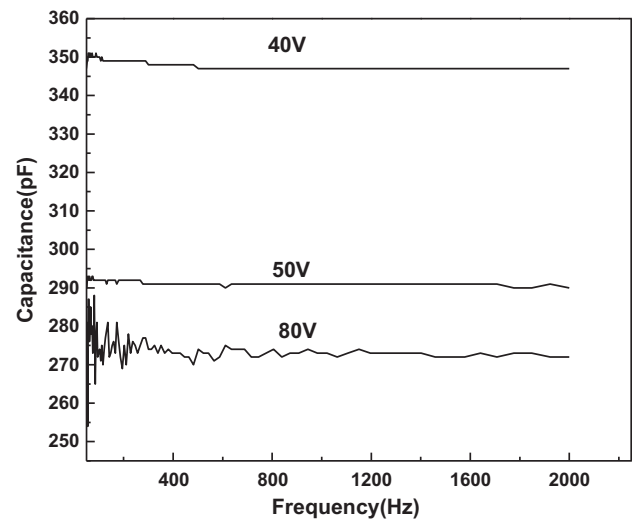


Fig. 5. Capacitance of porous aluminium coated with RTV silicone rubber as a function of frequency and anodising voltage.

However, when the pores become too large, water can penetrate into nano-pores producing a negative effect on wettability (see Fig. 3).

4. Conclusions

A superhydrophobic surface was prepared using two inexpensive industrial processes: anodization of the surface in phosphoric acid and spin coating of the anodized surface by RTV silicone rubber. SEM images showed that higher anodising voltage led to the larger pore diameter. The regularity of pore arrangement as well as the size of well-ordered domains increases with increasing anodising voltage. Bird's nest and beehive structures were found on 50 V and 80 V anodised surfaces. Study of water contact angles showed the best result for wettability in the case of 50 V anodising voltage. Freezing time was considerably improved for the elaborated superhydrophobic surfaces compared to those obtained by RTV coating on polished Al surfaces. Nevertheless, our study showed an important reduction in water static contact angle and increase in contact angle hysteresis for superhydrophobic surface at cold temperatures below 0°C. It was also found that increasing anodising voltage caused a reduction of the capacitance of superhydrophobic anodized surfaces.

Acknowledgements

This work was carried out within the framework of the NSERC/Hydro-Quebec/UQAC Industrial Chair on Atmospheric Icing of Power Network Equipment (CIGELE) and the Canada Research Chair on Engineering of Power Network Atmospheric Icing (INGIVRE) at Université du Québec à Chicoutimi. The authors would like to thank the CIGELE partners (Hydro-Québec, Hydro One, Réseau Transport d'Électricité (RTE) and Électricité de France (EDF), Alcan Cable, K-Line Insulators, Tyco Electronics, Dual-ADE, and FUQAC) whose financial support made this research possible. The authors also are grateful to Hélène Grégoire (National Research Council Canada, ATC, Saguenay) for SEM analysis.

References

- [1] F. Wang, C. Li, Lv Yuzhen, F. Lv, Y. Du, Ice accretion on superhydrophobic aluminium surfaces under low-temperature conditions, *Cold Regions Sci. Technol.* 62 (2010) 29–33.

- [2] Z.L. Jiang, J.Z. Lu, H.C. Lei, F.Y. Huang, Analysis of the causes of tower collapses in Hunan during the 2008 ice storm, *High Voltage Eng.* 34 (11) (2008) 2468–2474.
- [3] M. Farzaneh, *Atmospheric Icing of Power Networks*, Springer, Berlin, 2008, p. 381.
- [4] S.A. Kulinich, M. Farzaneh, How wetting hysteresis influences ice adhesion strength on superhydrophobic surfaces, *Langmuir* 25 (2009) 8854–8856.
- [5] S.A. Kulinich, M. Farzaneh, Ice adhesion on super-hydrophobic surfaces, *Appl. Surf. Sci.* 255 (2009) 8153–8157.
- [6] S.A. Kulinich, M. Farzaneh, On ice-releasing properties of rough hydrophobic coatings, *Cold Regions Sci. Technol.*, doi:10.1016/j.coldregions.2010.01.001.
- [7] R. Menini, M. Farzaneh, Elaboration of Al₂O₃/PTFE icephobic coatings for protecting aluminum surfaces, *Surf. Coat. Technol.* 203 (2009) 1941–1946.
- [8] Y. Liu, X. Chen, J.H. Xin, Super-hydrophobic surfaces from a simple coating method: a bionic nanoengineering approach, *Nanotechnology* 17 (2006) 3259–3263.
- [9] Z.P. Zhang, Y.H. Qi, Y. Zhang, G.K. Mo, J.Z. Wang, Investigation of Super-Hydrophobic Coatings with Hierarchical Structures Surface on Mild Steel, *Materials Science forum* 654–656 (2010) 1900–1903.
- [10] Q. BT, S. ZQ, Fabrication of superhydrophobic surfaces by dislocation-selective chemical etching on aluminum, copper, and zinc substrates, *Langmuir* 21 (2005) 9007–9009.
- [11] Z. Chen, Y. Guo, S. Fang, A facial approach to fabricate superhydrophobic aluminum surface, *Surf. Interface Anal.* 42 (2010) 1–6.
- [12] Z. Guo, F. Zhou, J. Hao, W. Liu, Stable biomimetic super-hydrophobic engineering materials, *J. Am. Chem. Soc.* 127 (2005) 15670–15671.
- [13] X. Fu, X. He, Fabrication of super-hydrophobic surfaces on aluminum alloy substrates, *Appl. Surf. Sci.* 255 (2008) 1776–1781.
- [14] Y. Huang, H. Shih, H. Huang, J. Daugherty, S. Wu, S. Ramanathan, C. Chang, F. Mansfeld, Evaluation of the corrosion resistance of anodized aluminum 6061 using electrochemical impedance spectroscopy (EIS), *Corr. Sci.* 50 (2008) 3569–3575.
- [15] R. Jafari, R. Menini, M. Farzaneh, Superhydrophobic and icephobic surfaces prepared by RF-sputtered polytetrafluoroethylene coatings, *Appl. Surf. Sci.* 257 (2010) 1540–1543.
- [16] J. Ye, Q. Yin, Y. Zhou, Superhydrophilicity of anodic aluminum oxide films: from “honeycomb” to “bird’s nest”, *Thin Solid Films* 517 (2009) 6012–6015.
- [17] G.D. Sulka, K.G. Parkola, Anodising potential influence on well-ordered nanostructures formed by anodisation of aluminum in sulphuric acids, *Thin solid Films* (2006) 338–345.
- [18] G. Momen, M. Farzaneh, Survey of micro/nano filler use to improve silicone rubber for outdoor insulators, *Rev. Adv. Mater. Sci.* 27 (2011) 14–34.
- [19] J. Kim, M.K. Chaudhury, M.J. Oweny, Diffusion of low molecular weight. Siloxane from bulk to surface, *J. Colloid. Interface Sci.* 226 (2000) 231–236.
- [20] M. Callies, Y. Chen, F. Marty, A. Pépin, D. Quéré, *Microelectron. Eng.* 78–79 (2005) 100–105.
- [21] G.Q. Ding, R. Yang, J.N. Ding, N.Y. Yuan, Y.Y. Zhu, Fabrication of porous anodic alumina with ultrasmall nanopores, *Nanoscale Res. Lett.* 5 (2010) 1257–1263.
- [22] L. Yin, Q. Xia, J. Xue, S. Yang, Q. Wang, Q. Chen, In situ investigation of ice formation on surfaces with representative wettability, *Appl. Surf. Sci.* 256 (2010) 6764–6769.
- [23] R. Karmouch, G.G. Ross, Experimental study on the evolution of contact angles with temperature near the freezing point, *J. Phys. Chem. C* 114 (2010) 4063–4066.
- [24] I.A. Ryzhkin, V.F. Petrenko, Physical mechanisms responsible for ice adhesion, *J. Phys. Chem. B* 101 (1997) 6267–6270.
- [25] V.F. Petrenko, R.W. Whitworth, *Physics of Ice*, Oxford University press, Oxford, 1999.